Electronic Supplementary Material (ESI) for Chemical Communications.

Supporting Information

Nanoscopic hydrophilic/hydrophilic phase-separation well below the LCST of Polyphosphoesters

Johannes Hunold,[a] Thomas Wolf,[b] Frederik R. Wurm[b] and Dariush Hinderberger*[a]

[a] Institut für Chemie, Martin-Luther-Universität Halle-Wittenberg, Von-Danckelmann-Platz 4, 06120 Halle (Saale), Germany. E-mail: dariush.hinderberger@chemie.uni-halle.de

[b] Max-Planck-Institut für Polymerforschung, Ackermannweg 10, 55128 Mainz, Germany.

1. Experimental methods and polymer characterization

Materials: The polymers investigated in this study were prepared according to a procedure in ref. 1. TEMPO (99%, purified by sublimation) as well as Dulbecco's Phosphate Buffered Saline D8662 (DPBS) were purchased from Sigma-Aldrich and used as received. For all sample preparations only ultrapure water (Milli-Q®, Merck Millipore) was used.

Turbidity measurements: For turbidity measurements the Litesizer™ 500 (Anton Paar, Graz, Austria) with a 40 mW semiconductor laser (λ = 658 nm) and low volume quarz cuvettes (50 µL, Hellma Analytics) were used. All measurements were performed with a detection angle of 175° and an automatic configuration (filter and focus) of the heatable optical bench. The temperature was changed in steps of 2 °C with an equilibration time of 2 min.

CW EPR spectroscopy: CW EPR spectra were measured with the benchtop EPR spectrometer MiniScope MS400 (Magnettech, Berlin, Germany) at X-band ($\nu \approx 9.4$ GHz). For this purpose, micropipettes (BLAUBRAND® intraMARK, Wertheim, Germany) were filled with about 15–20 µL of the sample (15 mg mL^{-1} polymer solution with 0.2 mM TEMPO in DPBS buffer), capped with capillary tube sealant (CRITOSEAL® Leica) and placed into the spectrometer. For all EPR measurements a magnetic field sweep of 10 mT centered on 336 mT and a scan time of 100 s were used. Values of microwave power and modulation amplitude were 8 mW and 0.02 mT respectively. The frequency counter RACAL DANA (model 2101, Neu-Isenburg, Germany) was used to record the exact microwave frequencies and temperatures were controlled with the Temperature Controller H03 (Magnettech, Berlin, Germany) with an accuracy of ± 0.25 °C. After each temperature change, an equilibration time of 2 min was maintained.

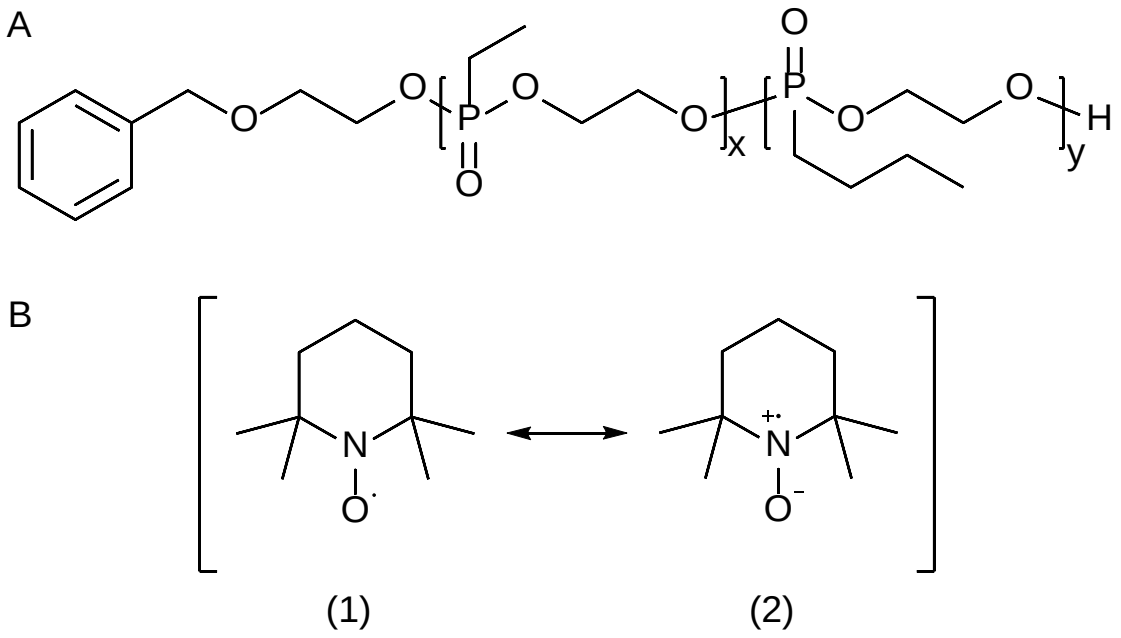

Chart S1 Structural formulas of the compounds used in this work. A) General structure of the investigated PPE copolymers with x = 33 and y = 76 for P(Et_{33}-co-$n$$Bu_{76}$) or x = 24 and y = 27 for P(Et_{24}-co-$n$$Bu_{27}$) (see Table S1). B) Mesomeric resonance structures (1) and (2) of TEMPO for describing the radical bond state in which the unpaired electron is located in the π-bond between nitrogen N and oxygen O.

Table S1 Characterization of the investigated PPE copolymers.

polymer name	x	y	w_x [%]	w_y [%]	M_n [g mol^{-1}][a)]	$Đ$[a)]	T_{cp} [°C]	T_{EPR} [°C]
P(Et_{33}-co-$n$$Bu_{76}$)	33	76	30	70	17000	1.30	26	18
P(Et_{24}-co-$n$$Bu_{27}$)	24	27	47	53	7700	1.29	50	42

x: number of monomer units with ethyl side chain; y: number of monomer units with n-butyl side chain; w_x: percentage of monomer units with ethyl side chain; w_y: percentage of monomer units with n-butyl side chain; M_n: molecular weight; $Đ$: molecular weight distribution; T_{cp}: macroscopic cloud point temperature; T_{EPR}: EPR-derived nanophase separation temperature; [a)] Data taken from ref. 1.

2. EPR simulation process

Spectral simulations of the measured EPR spectra were performed with home-written MATLAB scripts using the simulation function "chili" of the software package EasySpin (v. 5.2.20), developed by Stoll and Schweiger.[2] This simulation approach is based on the Schneider-Freed theory, solving the Schrödinger equation for slow tumbling nitroxides.[3]

The simulation parameters itself were adjusted by an iterative manual procedure until the root-mean-square deviation (RMSD) of the difference between experimental and simulated spectrum was sufficiently low (i.e. RMSD < 1%). The diagonal **g**- and hyperfine splitting **A**-tensor (**g** = [g_{xx} g_{yy} g_{zz}]; **A** = [A_{xx} A_{yy} A_{zz}]) were determined by their three main components along the three principal room directions (Fig. S14). As initial values for **g** and **A** of the TEMPO radical, suitable literature data were used, each slightly adapted to the system under investigation.[4] Within a sample, g_{yy} and g_{zz} were kept constant during the simulation process, since the X-band spectra are mainly influenced by the g_{xx}-value.

However, it should also be mentioned that the obtained *g*-values (Fig. S12) are just of a qualitative character and have no real quantitative significance, as they are based only on X-band EPR measurements. For a truly quantitative statement, high-field EPR measurements, e.g. at W-band ($\nu \approx 95$ GHz), would be necessary. The isotropic values g_{iso} and a_{iso} can be calculated from the simulated tensor data with Eq. (S1) and (S2).

$$g_{iso} = \frac{1}{3}\left(g_{xx} + g_{yy} + g_{zz}\right) \tag{S1}$$

$$a_{iso} = \frac{1}{3}\left(A_{xx} + A_{yy} + A_{zz}\right) \tag{S2}$$

The calculation of the rotation correlation time τ_c using the rotational diffusion tensor $\mathbf{D} = [D_{xx}\ D_{yy}\ D_{zz}]$ was based on an axial rotation model (i.e. $D_{xx} < D_{yy} = D_{zz}$) according to the following equation.

$$\tau_c = \frac{1}{6\sqrt[3]{D_{xx}D_{yy}D_{zz}}} = \frac{1}{6\sqrt[3]{D_{xx}D_{zz}^2}} \tag{S3}$$

Besides the influence of τ_c on the spectral line width, an additional convolutional line broadening was considered in the simulations with EasySpin. This so-called heterogeneous line broadening is mainly due to unresolved hyperfine couplings between electron and nuclear spins (usually ^{1}H) and depends among other things on the type of solvent, the oxygen content of the solution and the spin probe concentration. The method implemented in EasySpin to include this additional line broadening in addition to the rotational dynamics is not based on any physical model.

For the Euler angle β, which describes the orientation of **D** in the molecular coordinate system of the nitroxide radical (equal to the coordinate system of the magnetic parameters **g** and **A**; see Fig. S14), a value of 50° was selected.

3. EPR spectra and simulations

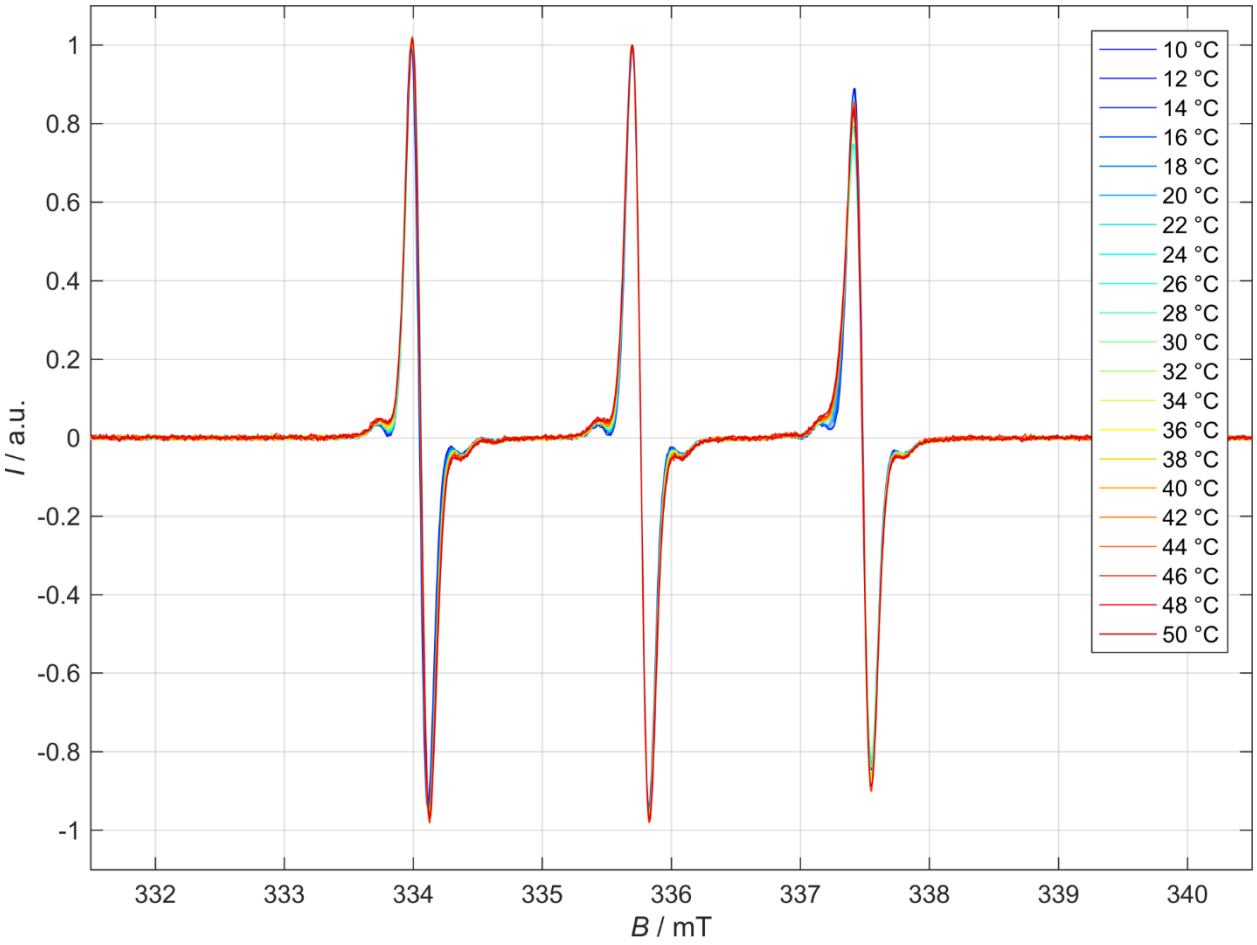

Fig. S1 CW EPR spectra of 15 mg mL^{-1} P(Et$_{33}$-co-*n*Bu$_{76}$) with 0.2 mM TEMPO in DPBS buffer at temperatures *T* between 10 °C and 50 °C. For a better comparability of the spectra with respect to polarity (i.e. changes of a_{iso}) and line shape changes, they were manually centered on the zero crossing of the center-field signal.

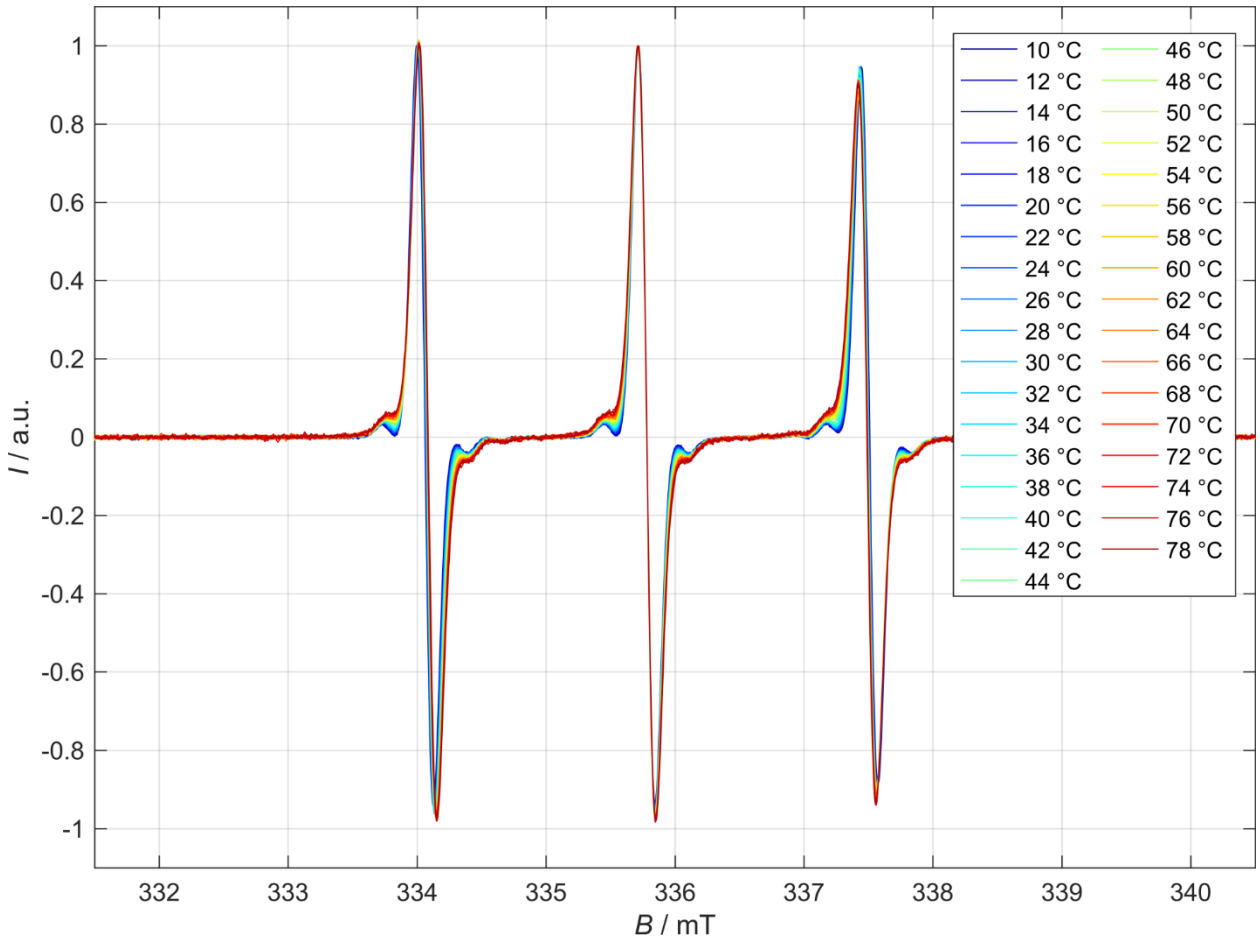

Fig. S2 CW EPR spectra of 15 mg mL^{-1} P(Et$_{24}$-co-*n*Bu$_{27}$) with 0.2 mM TEMPO in DPBS buffer at temperatures *T* between 10 °C and 78 °C. For a better comparability of the spectra with respect to polarity (i.e. changes of a_{iso}) and line shape changes, they were manually centered on the zero crossing of the center-field signal.

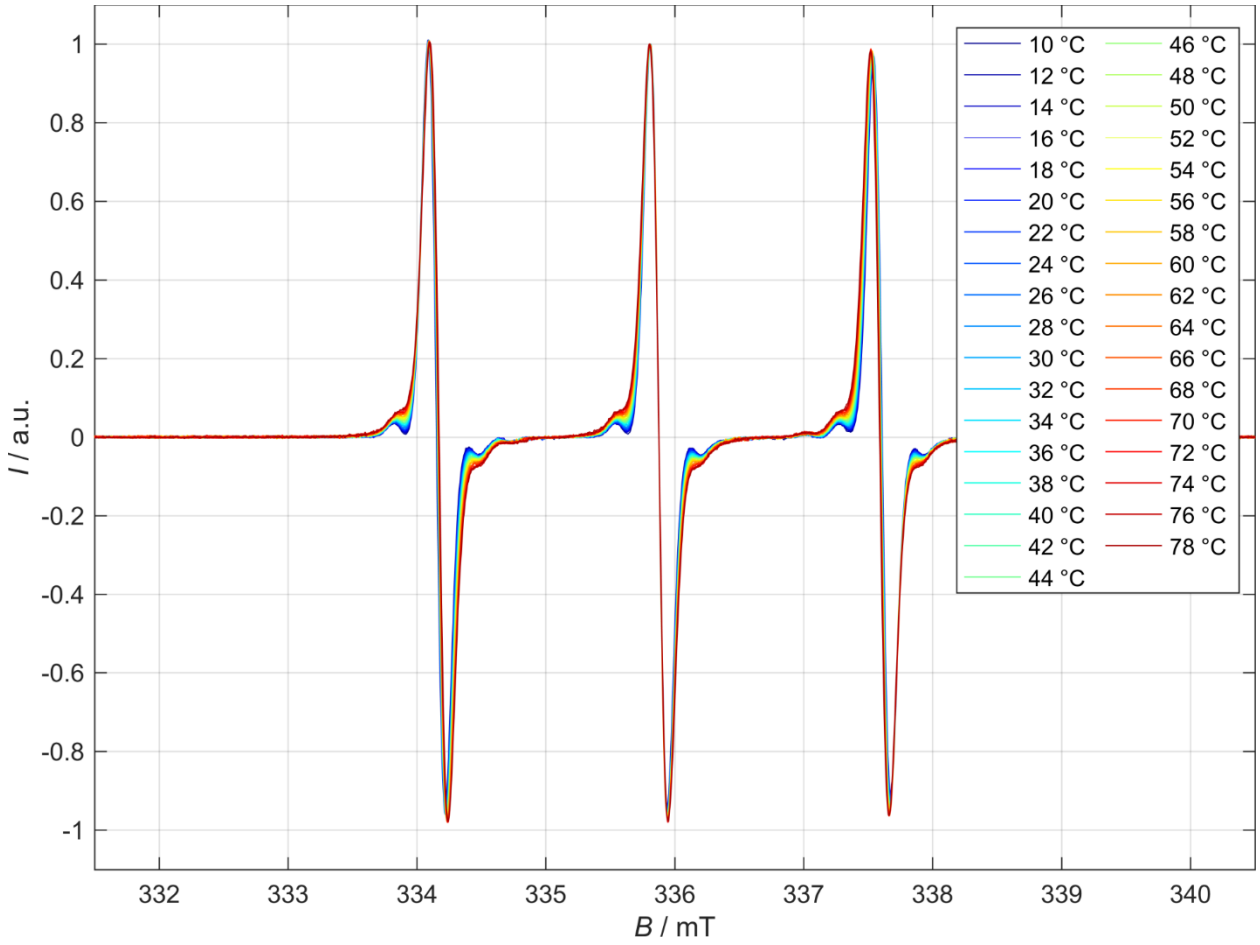

Fig. S3 CW EPR spectra of a 0.2 mM TEMPO reference sample with DPBS buffer at temperatures *T* between 10 °C and 78 °C. For a better comparability of the spectra with respect to polarity (i.e. changes of a_{iso}) and line shape changes, they were manually centered on the zero crossing of the center-field signal.

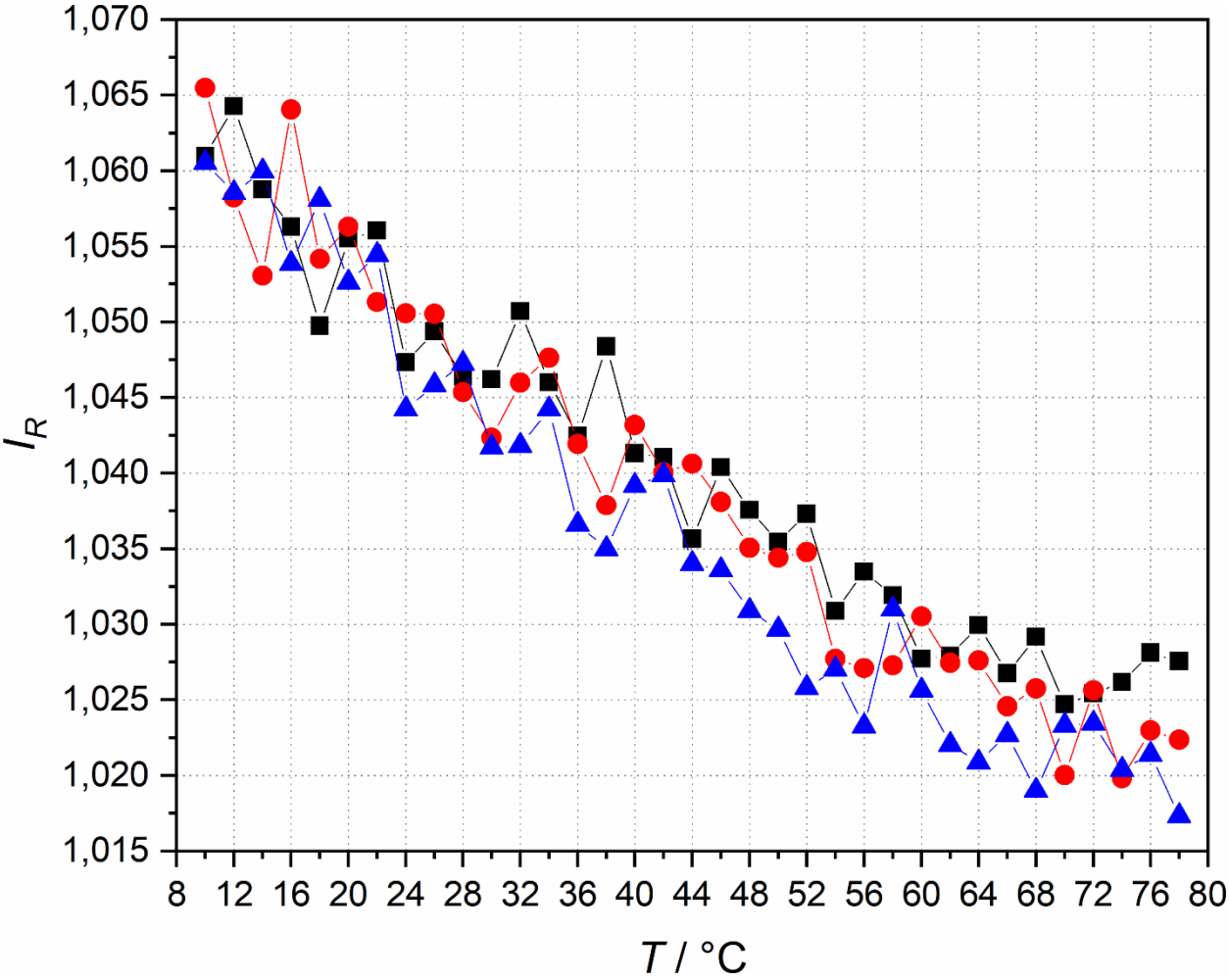

Fig. S4 Intensity ratio $I_R = |I_+/I_-|$ of low-field (black squares), center-field (red circles) and high-field (blue triangles) signal as a function of temperature T for a 0.2 mM TEMPO reference sample with DPBS buffer. The almost linear decrease of I_R with increasing T observed for all three signals shows the increasingly isotropic character of the CW EPR spectra, as the TEMPO probes rotates faster (i.e. more uniformly or isotropic) at higher temperatures. A value of $I_R = 1$ would correspond to a perfect signal symmetry, as the intensity above (I_+) and below (I_-) the zero line would be exactly the same.

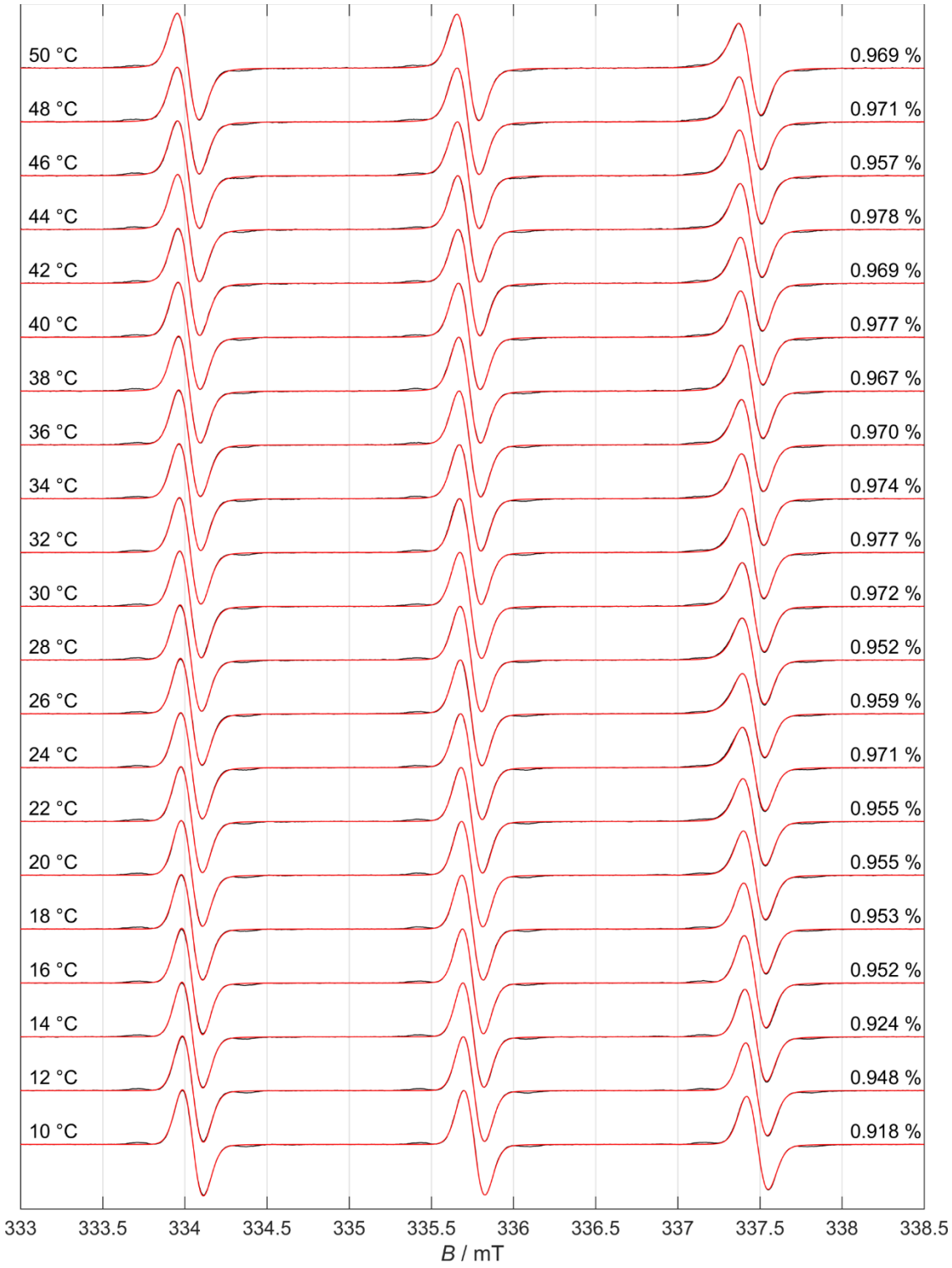

Fig. S5 EPR spectral simulations of 15 mg mL^{-1} P(Et$_{33}$-co-*n*Bu$_{76}$) with 0.2 mM TEMPO in DPBS buffer, with corresponding temperature *T* (left) and RMSD value (right). Experimental spectra are shown in black and simulations in red.

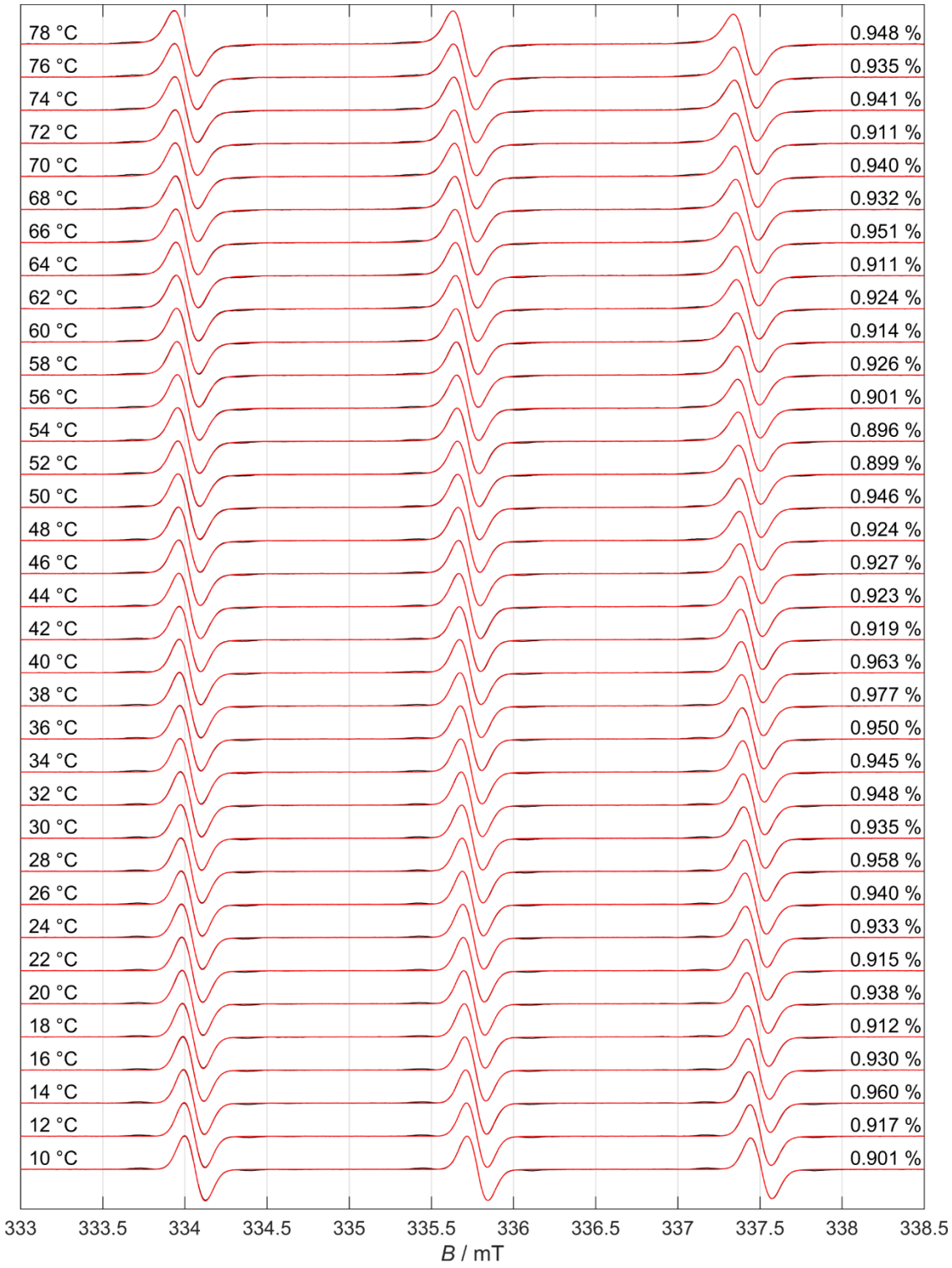

Fig. S6 EPR spectral simulations of 15 mg mL^{-1} P(Et$_{24}$-co-*n*Bu$_{27}$) with 0.2 mM TEMPO in DPBS buffer, with corresponding temperature *T* (left) and RMSD value (right). Experimental spectra are shown in black and simulations in red.

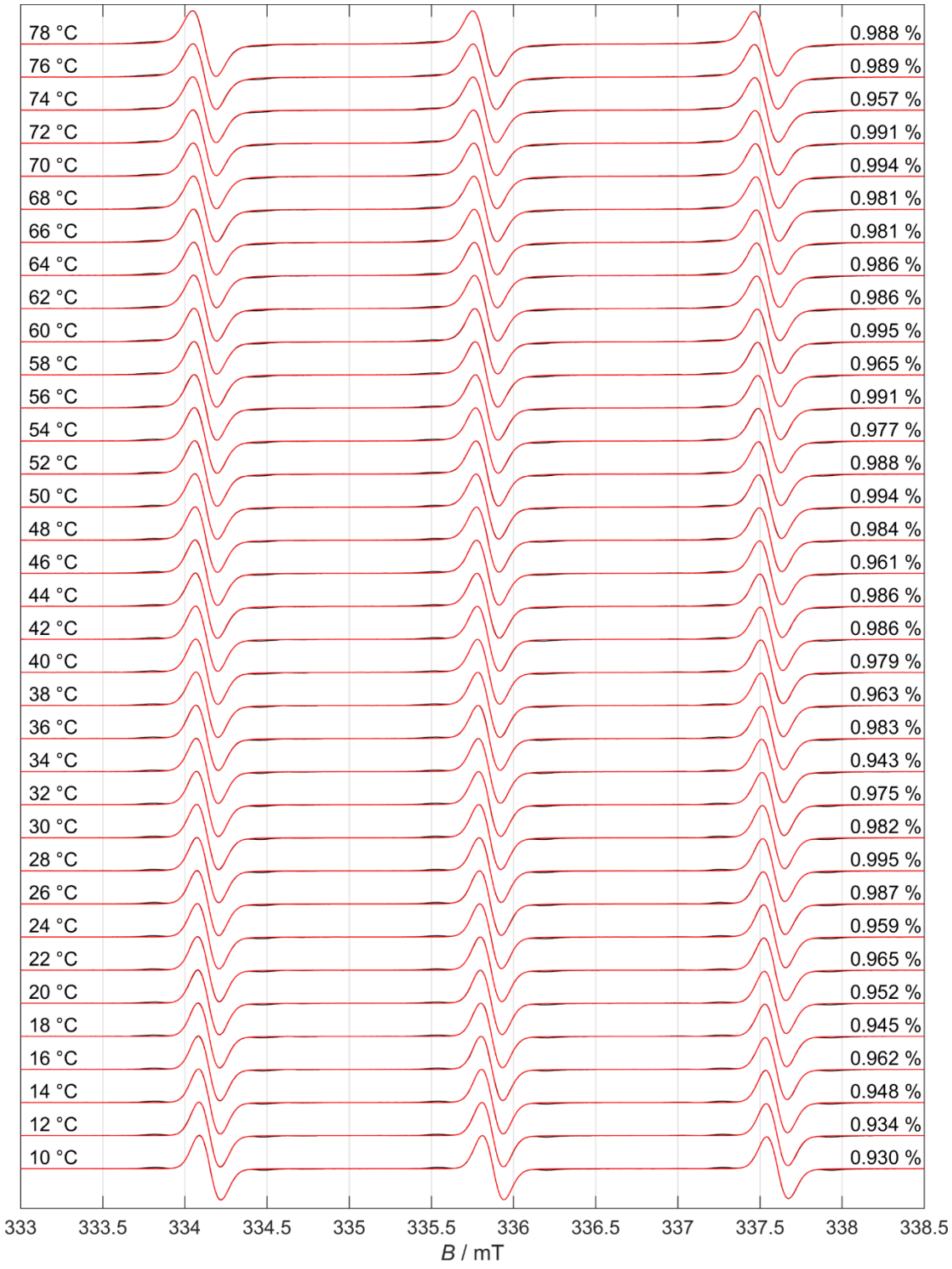

Fig. S7 EPR spectral simulations of a 0.2 mM TEMPO reference sample with DPBS buffer, with corresponding temperature T (left) and RMSD value (right). Experimental spectra are shown in black and simulations in red.

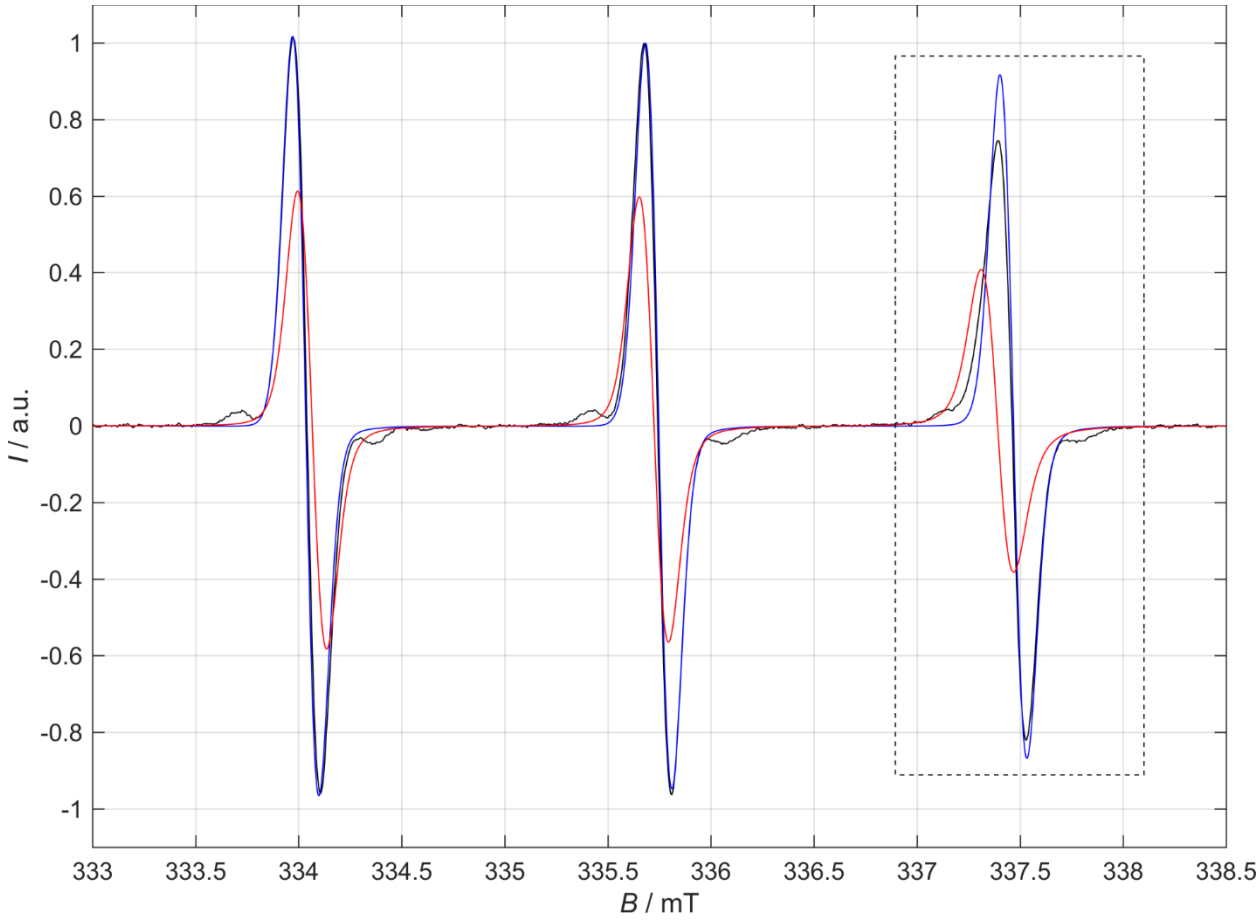

Fig. S8 Measured EPR spectrum (black) of 15 mg mL^{-1} P(Et_{33}-co-*n*Bu_{76}) with 0.2 mM TEMPO in DPBS buffer at 26 °C, with simulated hydrophilic (blue) and hydrophobic (red) spin probe species. The signal intensity *I* of the hydrophobic component (red curve) was multiplied by a factor of 50 for better visibility. The *B*-field region of the high-field signal framed with a dashed box is displayed enlarged in Fig. S9.

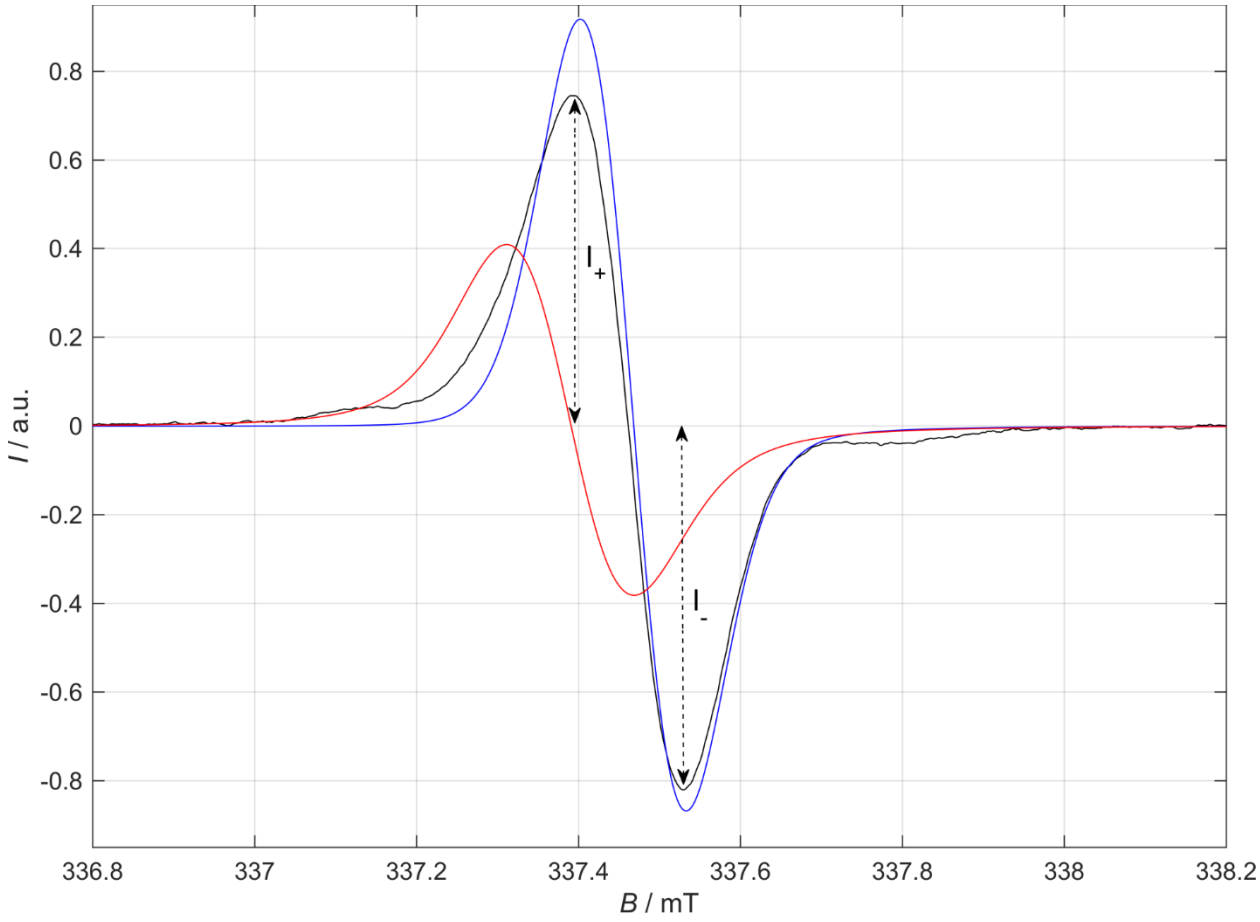

Fig. S9 Enlarged B-field region of the high-field signal from Fig. S8 (dashed box) with measured EPR spectrum (black) as well as the simulated hydrophilic (blue) and hydrophobic (red) spin probe species. The dashed black double arrows show the intensity above (I_+) and below (I_-) the zero line, which are used for the calculation of the intensity ratio $I_R = |I_+/I_-|$. Due to the slightly lower environmental polarity and the thus smaller a_{iso} value of the hydrophobic spin probe species (red curve), its high-field signal minimum shifts below the high-field signal maximum of the hydrophilic probe species (blue curve). The resulting stronger decrease of I_+ compared to I_- leads in sum to a decrease of the intensity ratio I_R of the actually measured spectrum (black curve), which is a weighted superposition of the single simulated spectra (blue and red curve).

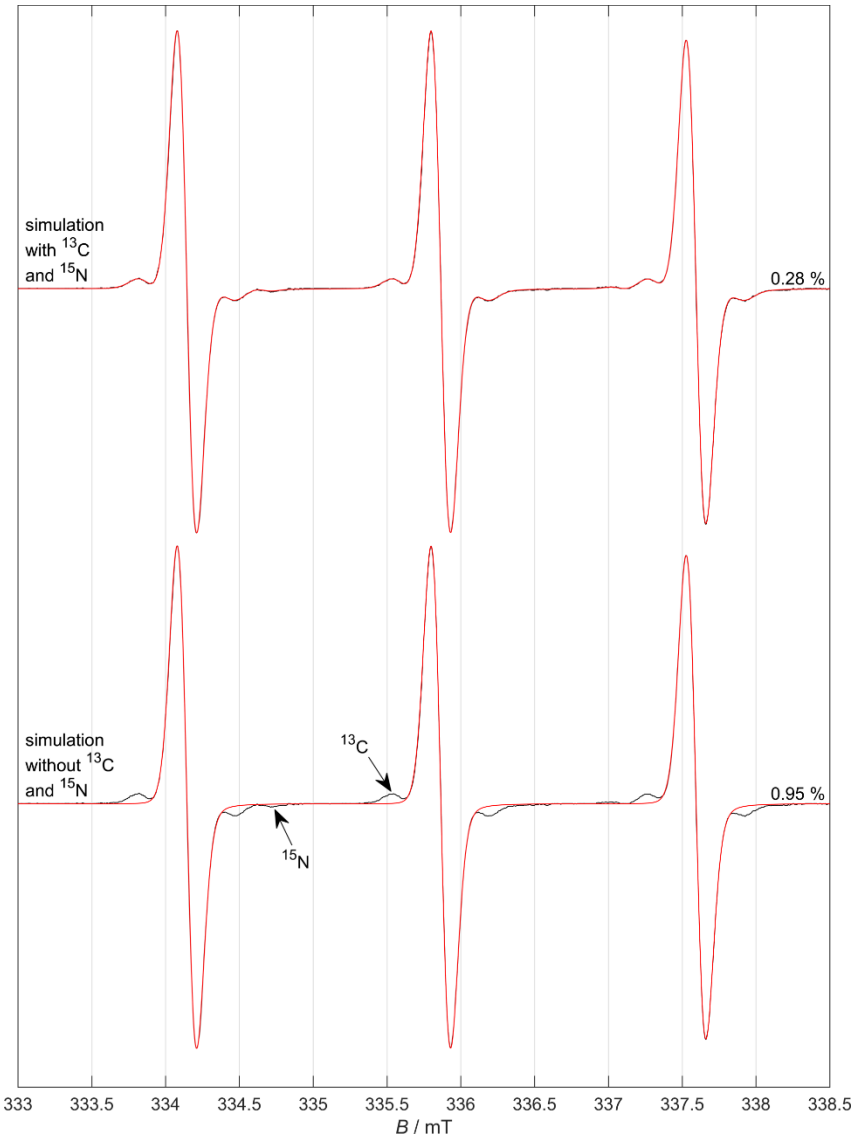

Fig. S10 EPR spectral simulations of 0.2 mM TEMPO in DPBS buffer at 20 °C, with (top) and without (bottom) consideration of ^{13}C and ^{15}N as well as the respective RMSD value (right). Experimental spectra are shown in black and simulations in red. It can be seen that by including the ^{13}C (natural abundance $\approx 1.11\%$) and ^{15}N (natural abundance $\approx 0.36\%$) isotopes in the simulation approach, the RMSD values can be reduced at least by a factor of about 3. However, since disregarding the ^{13}C and ^{15}N nuclei does not influence the simulation results in terms of their validity with regard to the polymer phase separation process and leads to a significant reduction of the simulation computing time, they were neglected in all other simulations shown in this paper.

4. Simulation results and other figures

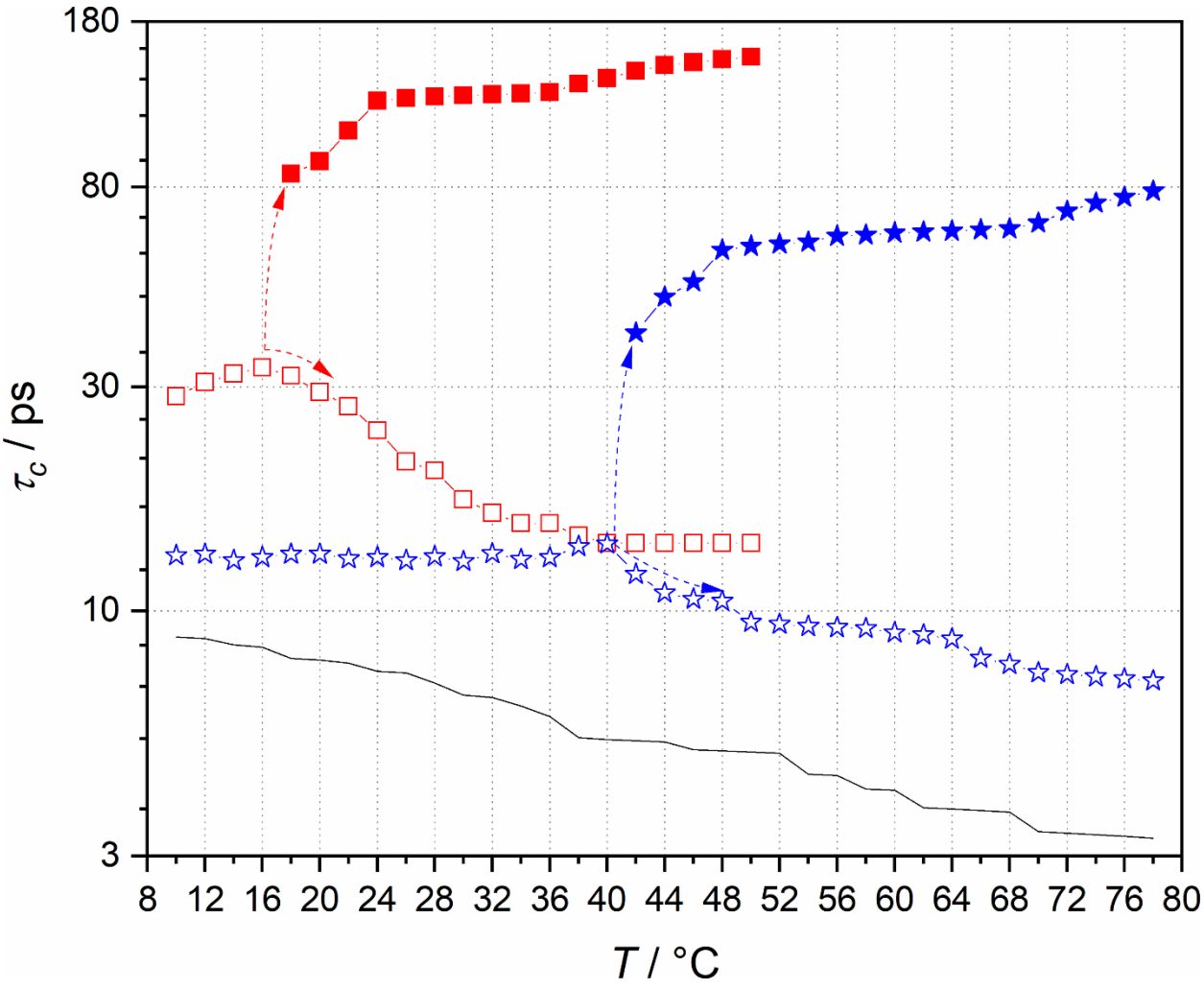

Fig. S11 Rotation correlation time τ_c as a function of temperature T for P(Et_{33}-co-$n$$Bu_{76}$) (red squares) and P($Et_{24}$-co-$n$$Bu_{27}$) (blue stars), at polymer concentrations of 15 mg mL^{-1} in DPBS buffer. The open symbols indicate the hydrophilic species, while the filled icons represent the hydrophobic component. Data from a 0.2 mM TEMPO reference sample with DPBS buffer are shown as black line. The red and blue dashed arrow are meant as guides to the eye. Please note the logarithmic scaling of the τ_c-axis.

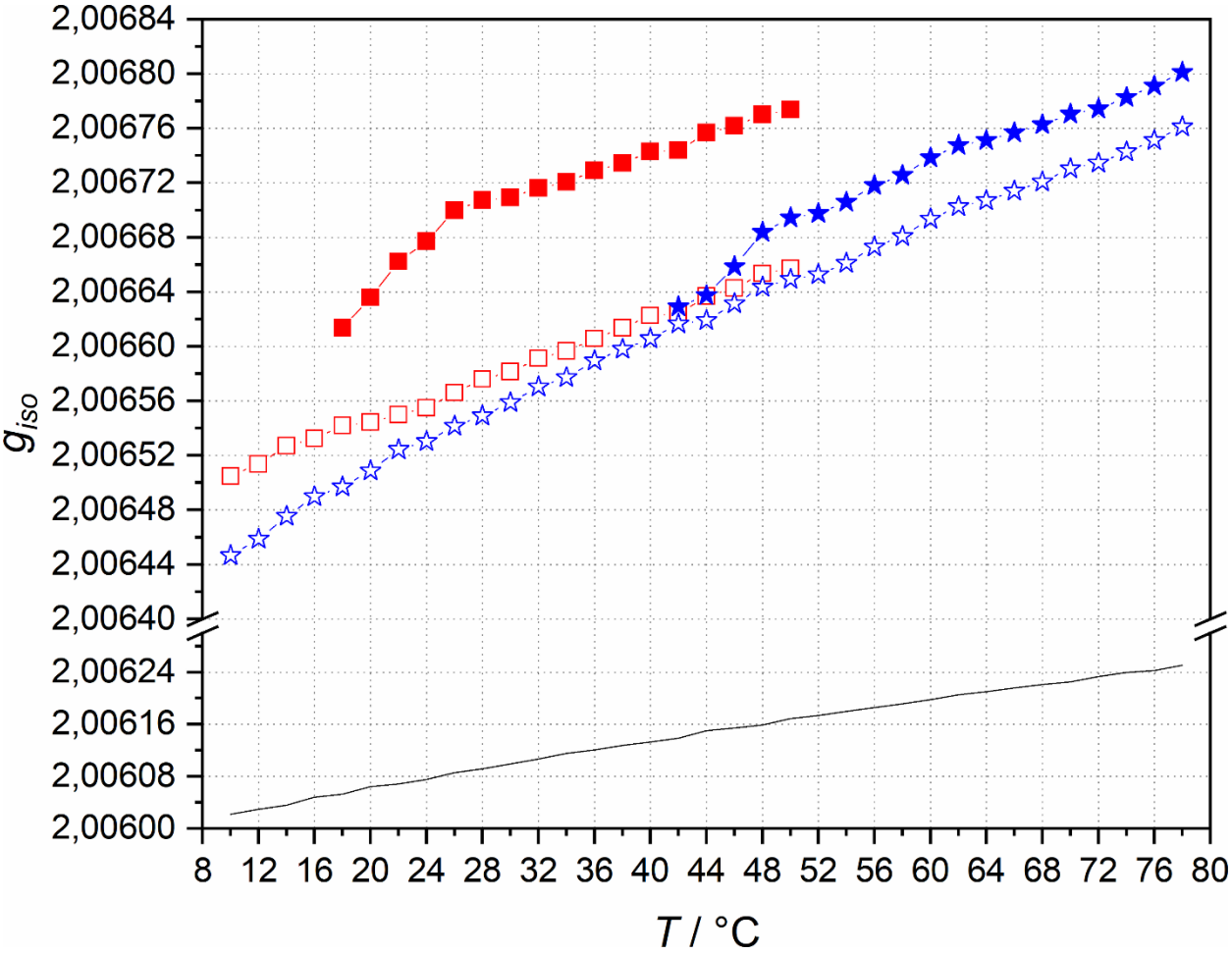

Fig. S12 Isotropic Landé *g*-factor g_{iso} as a function of temperature *T* for P(Et_{33}-co-*n*Bu_{76}) (red squares) and P(Et_{24}-co-*n*Bu_{27}) (blue stars), at polymer concentrations of 15 mg mL^{-1} in DPBS buffer. The open icons indicate the hydrophilic probe species, while the filled symbols represent the hydrophobic component. Data from a 0.2 mM TEMPO reference sample with DPBS buffer are shown as black line. Please note the interruption of the g_{iso}-axis.

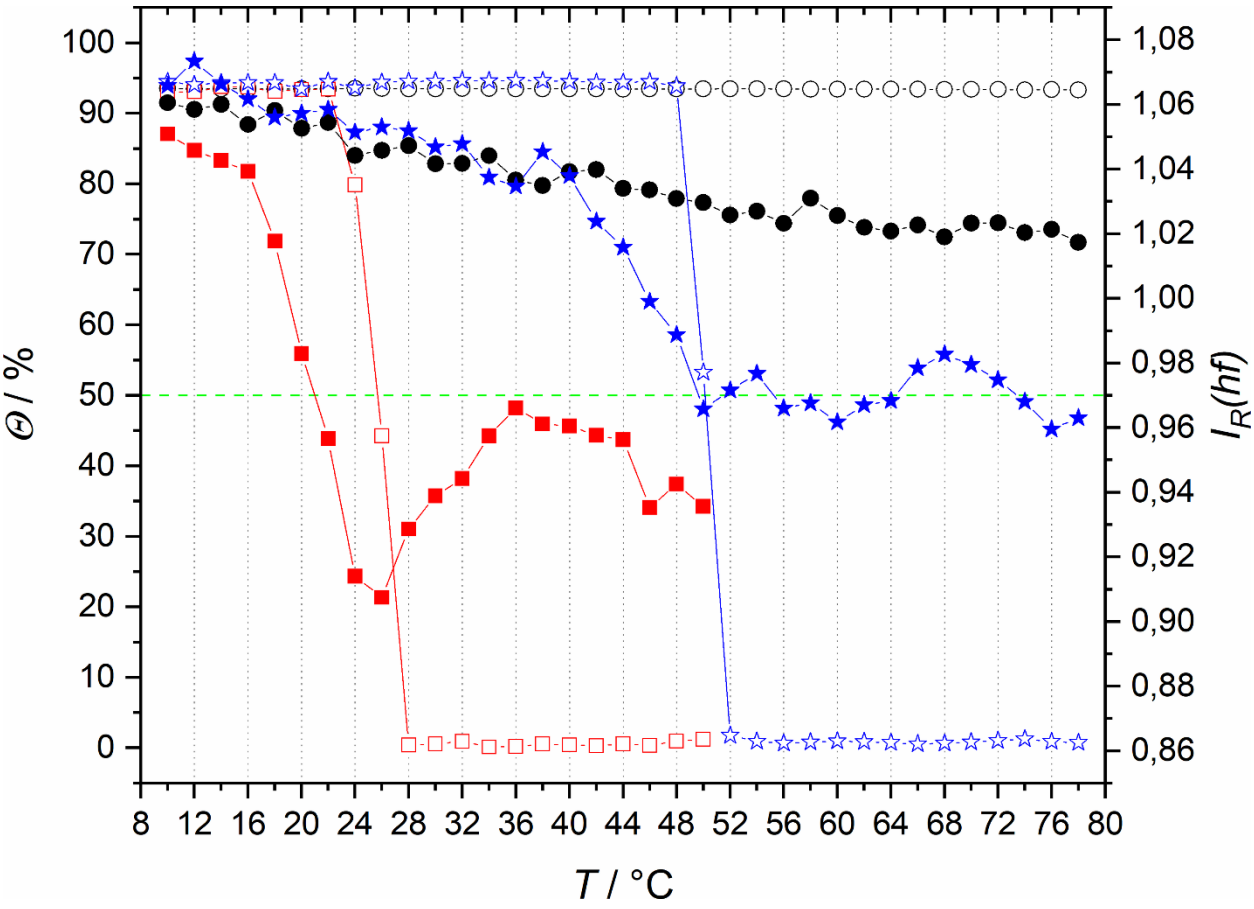

Fig. S13 Transmittance Θ (left axis) and intensity ratio of high-field signal $I_R(hf)$ (right axis) as a function of temperature T for P(Et_{33}-co-nBu$_{76}$) (red squares) and P(Et_{24}-co-nBu$_{27}$) (blue stars) in DPBS buffer at polymer concentrations of 15 mg mL^{-1}, as well as a 0.2 mM TEMPO reference sample also in DPBS buffer (black circles). The open symbols with dashed line belong to the left Θ-axis, while the filled icons with solid line are related to the right $I_R(hf)$-axis. The intersections of the turbidity curves (open symbols and dashed line) with the green dashed line at Θ = 50% were used to determine the given macroscopic cloud point temperatures T_{cp}.

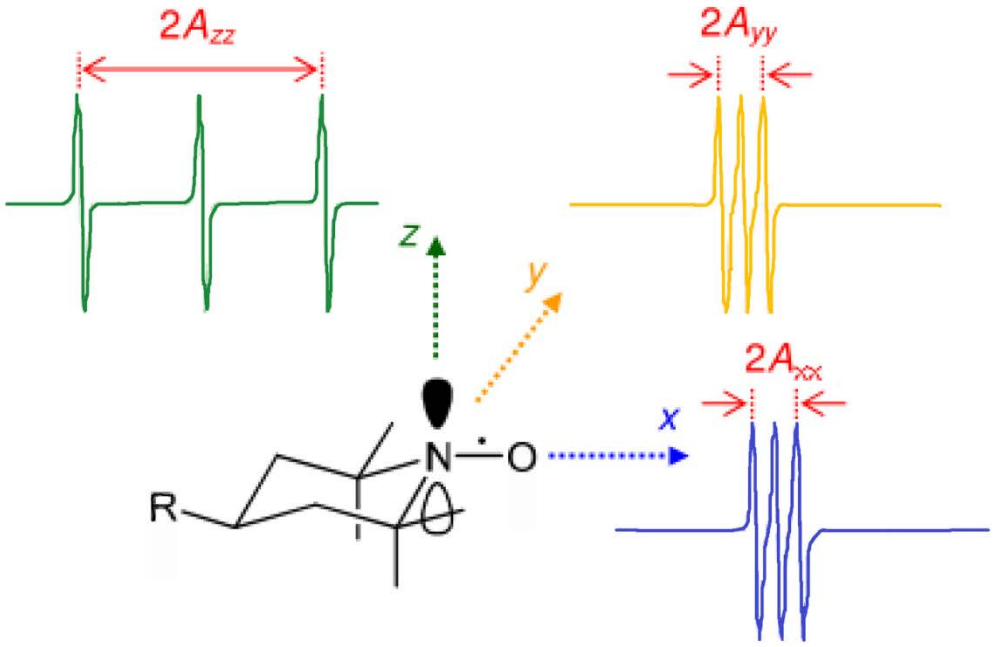

Fig. S14 Illustration of the general structure of nitroxides (TEMPO: R = H) and their molecular coordinate system, as well as the hypothetical CW EPR spectra with the respective hyperfine splitting tensor component (A_{xx}, A_{yy}, A_{zz}), by rotation of the spin probe along the three principal room directions. The z-axis is aligned along the π-bond using the shown p_z-orbital of the nitrogen atom N, while the x-axis points in the direction of the N–O σ-bond. The y-axis is perpendicular to the x-z-plane and completes the Cartesian coordinate system. Figure adapted from ref. 5.

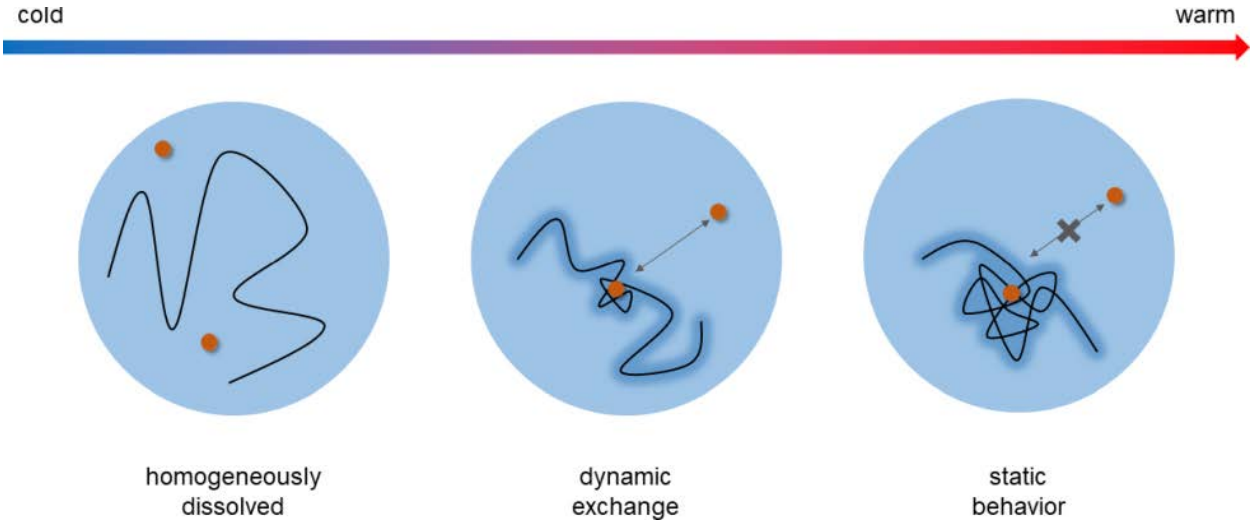

Fig. S15 Schematic depiction of the nanoscale processes described in the main text. Figure adapted from ref. 6.

References

1 T. Wolf, J. Hunold, J. Simon, C. Rosenauer, D. Hinderberger and F. R. Wurm, *Polym. Chem.*, 2018, **9**, 490.

2 S. Stoll and A. Schweiger, *J. Magn. Reson.*, 2006, **178**, 42.

3 D. J. Schneider and J. H. Freed, *Biol. Magn. Reson.*, 1989, **8**, 1.

4 V. P. Timofeev, A. Yu. Misharin and A. Yu. Tkachev, *Biophysics*, 2011, **56**, 407.

5 D. Hinderberger, Polyelectrolytes and Their Counterions Studied by EPR Spectroscopy, Johannes Gutenberg-Universität Mainz, 2004.

6 D. Kurzbach, M. J. N. Junk and D. Hinderberger, *Macromol. Rapid Commun.*, 2013, **34**, 119.